5.1. Introduction

The potential application and miniaturization of electronic devices required high permittivity, low dielectric loss [Luo *et al*. (2016), Chon *et al*. (2010)] and temperature dependent remanent polarization which are essential parameters for the materials [Bhandari and Kumar (2015), Feng *et al*. (2015), Lee and Aksay (2001), Thakur and Gupta (2016)]. The hexagonal perovskite family displays variety of remarkable physical properties such as colossal magnetoresistance, superconductivity and high permittivity [Jordan and Battle (2003)]. The hexagonal perovskite having high dielectric constant such as $Ba_4YMn_3O_{11.5}$ [Kuang *et al*. (2006), Barbier *et al*. (2012)] and doping of copper at the site of manganese increase the dielectric properties [Barbier *et al*. (2013)]. The tolerance factor is greater than unity indicates the hexagonal perovskites structure [Sondena *et al*. (2007)]. The perovskite oxide, $BaTiO_3$ is a typical ferroelectric material belonging to tetragonal crystal system at room temperature [Wang *et al*. (2014)]. The high dielectric constant of $BaTiO_3$ is the main key for the ferroelectricity of the material in which the TiO_6 octahedra is slightly tilted from the Centre which is responsible for remanent polarization. On application of external electric field, the opposite shifting of Ti^{4+} and oxide ions results the good ferroelectric properties [Haertling (1999)]. The generation of electric polarization due to shift in the position of cations and anions due to pairing of electrons of B-site transition metal ions with vacant orbitals of neighboring oxide ions. Such type of polarizations and electronic heterogeneity of material is responsible for the dielectric and ferroelectric properties of $BaTiO_3$. Previous investigations showed that the doping in $BaTiO_3$ monitored the electrical properties due to formation of defects in solid crystal [Chen *et al*. (1997), Yu *et al*. (1997)]. The partial substitution of Ti^{4+} by Y^{3+} in $BaTiO_3$ acts as acceptor, the excess positive charge is balanced by creating oxygen vacancies (V_o'')

[Zhi *et al*. (1999)]. The ionic radii of Y^{3+} and Ti^{4+} is quite different but incorporation of yttrium at B-site takes place due to A/B ratio [Makovec *et al*. (2004)] which is greater than one. The duration of sintering, temperature and partial pressure are also responsible for the enhancement of dielectric and ferroelectric properties [Tsur *et al*. (2001)]. The continuous dependent of dielectric constant on temperature and frequency elucidate the concentration of yttrium doping in $BaTiO_3$ [Belous *et al*. (2005)].There are various chemical methods reported in literature for the synthesis of high dielectric constant ceramic materials having titanium at B-site of the various perovskite systems such as sol-gel, semi-wet, microwave heating, hydrothermal process, co-precipitation, flame synthesis and precursor solution techniques [Liu *et al*. (2007), Jha *et al*. (2003), Masingboon *et al*. (2008), Yu *et al.* (2008), Liu *et al.* (2008), Barbier *et al*. (2009),Li *et al*. (2012)]. The Ba-Y-Ti-O phase was first observed in the study of superconducting $YBa_2Cu_3O_7$ films on $SrTiO_3$ [Derk *et al*. (1988)]. The solid state reaction of $YBa_2Cu_3O_7$ and $SrTiO_3$ powder produced major phase of hexagonal unit cell having lattice parameter a = b = 5.928 Å, c = 29.514 Å and Z = 4. The assigned formula was $Ba_3YTi_2O_{8.5}$ or $Ba_6Y_2Ti_4O_{17}$ and the crystal structure was well described. It exhibits hexagonal 12-layer perovskite structure with space group $P6_3/mmc$ [Kuang *et al*. (2002)]. This mixed oxide ceramic exhibits ionic and hole conductivity [Ping and West (2002)]. The bulk conductivity of the ceramic was found to be $1.8 \times 10^{-3}\ \Omega^{-1}cm^{-1}$ at 700 ^{0}C and oxygen transport number was 0.35 over the temperature range 300 – 700 ^{0}C. In this chapter $Ba_6Y_2Ti_4O_{17}$ (BYTO) hexagonal perovskite was synthesized for the first time by semi-wet route using aqueous solution of metal nitrates and glycine as oxidant fuel along with solid TiO_2 as titanium source. The present synthesis method is simple in the comparison to solid-state method because there are several multiple steps are involved (i.e., intermediate grindings, drying etc.) to get precursor powder.

On the other hand, sol-gel methods make use of very costly alkoxides of titanium as Titanium source. The dielectric, ferroelectric and magnetic properties of BYTO ceramic in systematic way with the variation of temperature and frequencies are also discussed in this chapter.

5.2. Experimental

5.2.1. Materials synthesis

BYTO ceramic was synthesized by semi wet combustion route. The chemicals used are of analytical grade, $Ba(NO_3)_2$ (99 % Merck), $Y(NO_3)_3.6H_2O$ (99.8 %, Sigma-Aldrich), TiO_2 (99 % Merck) and glycine (99 %, Merck) were used after purity correction. In this method, the aqueous solutions of Ba^{2+}, Y^{3+} were taken in a beaker and mixed with solid TiO_2 powder in their stoichiometric amounts. Then the aqueous solution of glycine was added as per equivalent of metal ions in to the heterogeneous mixture. The obtained heterogeneous mixture was heated at 70 - 80 ^{0}C with continuous stirring until the formation of gel by evaporation of water and nitrogen in form of their oxides (brown NO_2). The resulting gel was burned with sooty flame in which glycine acts as oxidant fuel. The obtained fluffy solid mass was converted in to fine powder with the help of agate and mortar. The dry powder was calcined at 800 and 1000 ^{0}C at 8 and 12 h respectively. The resulting calcined powder was used to make cylindrical pellets with the help of PVA binder and finally sintered at 1400 ^{0}C for 24 h. After sintering, the pellets were polished with emery paper to make its surface smooth and silver paste was applied on both the sides of pellets to make its surface conducting.

5.2.2. Characterization and application of material

The dielectric measurement (PSM1735- NumetriQ U.K), PE loop measurement (PE loop tracer- Marine India), magnetic measurement was carried out with MPMS (SQUID Magnetometer Quantum design) at few selected temperatures. Dry precursor powder was used for thermal analysis (TG/DTA) (SII 6300 EXSTAR). The powder diffraction pattern of BYTO recorded by XRD (Rigaku Miniflex 600 Japan) with scan rate of 1°/min keeping step size 0.02. For the morphological study, the fractured surface of the pellet used for imaging in scanning electron microscopy (FEI NOVA NANOSEM 450), and its elemental composition was determined by energy dispersive X-ray spectroscopy (EDX). For surface roughness and height of particle the sample was characterized by Atomic Force Microscopy (Bruker, Dimension Edge with Scan Asyst). The bright field TEM image and electron diffraction patterns were recorded by transmission electron microscopy (TECHNAI G^2 TWIN) of ultrafine BYTO powdered ceramic.

5.3. Results and discussion

The differential thermal analysis (DTA) and thermo-gravimetric analysis (TGA) have been carried out to determine the calcination temperature of $Ba_6Y_2Ti_4O_{17}$ precursor powder at heating rate of 10°/min from room temperature to 950 ^{0}C as shown in Figure 5.1. The TG curve showed the two stage of weight loss, the first major weight loss of 29.9 % from the weight fraction of the BYTO precursor occurred in the temperature range of 100 – 750 ^{0}C due to elimination of residual water and combustion of remaining amount of glycine molecules present in precursor powder along with formation of intermediates ($BaCO_3$, Y_2O_3). The second stage which shows the weight loss of 26.9 % from 800 to 950 ^{0}C is due to the formation of

intermediate $BaTiO_3$, Ba_2TiO_4. These results also supported by powder XRD patterns of different calcination temperature of BYTO and the possible equations for the formation of intermediates were shown in equations (5.1 - 5.3). The temperature flow (°C/mg) supports the corresponding weight losses and formation of BYTO ceramic.

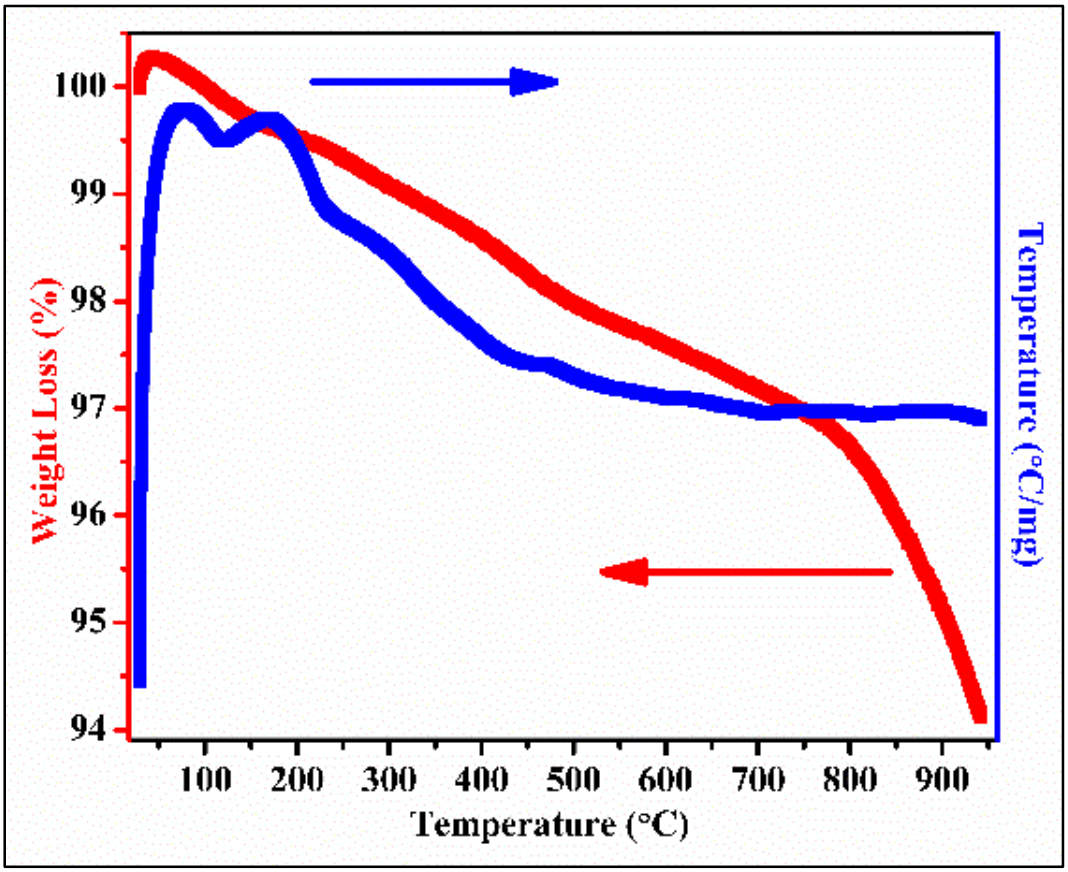

Figure 5.1 TG/DTA curve of precursor powder of $Ba_6Y_2Ti_4O_{17}$

$$BaCO_3 + TiO_2 \rightarrow BaTiO_3 + CO_2 \quad (5.1)$$

$$BaCO_3 + TiO_2 \rightarrow Ba_2TiO_4 \quad (5.2)$$

$$BaTiO_3 + BaCO_3 \rightarrow Ba_2TiO_4 + CO_2 \qquad (5.3)$$

Figure 5.2 shows the XRD pattern of BYTO calcined at 800 ^{0}C, 1000 ^{0}C and sintered at 1400 ^{0}C for 8, 12 and 24 h respectively. The XRD spectra of 800 ^{0}C clearly show the mixed phases of $BaCO_3$, Y_2O_3 and TiO_2 whereas XRD spectra of 1000 ^{0}C revels the formation of Ba_2TiO_4, $BaTiO_3$ and Y_2O_3 phases [Chen *et al*. (1996)].

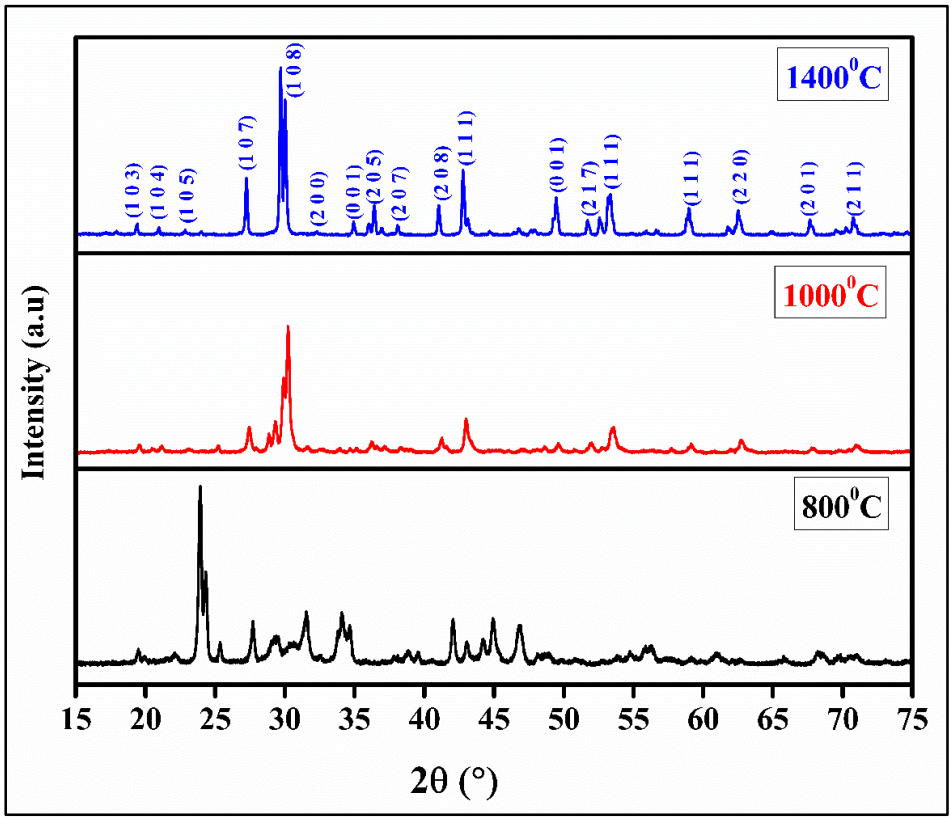

Figure 5.2 X-ray diffraction pattern of BYTO ceramic calcined at 800 ^{0}C, 1000 ^{0}C and sintered at 1400 ^{0}C for 24 h

The formation of single phase of BYTO was clearly observed at 1400 ^{0}C as per chemical reaction shown in equation (5.4). All the X-ray diffraction peaks were indexed with JCPDS (card no 43-0417).

$$2BaTiO_3 + Y_2O_3 + 2Ba_2TiO_4 \rightarrow Ba_6Y_2Ti_4O_{17} \quad (5.4)$$

To determine the hexagonal structure of BYTO ceramic, Rietveld refinement was performed on XRD data with space group $P6_3/mmc$ and is shown in Figure 5.3.

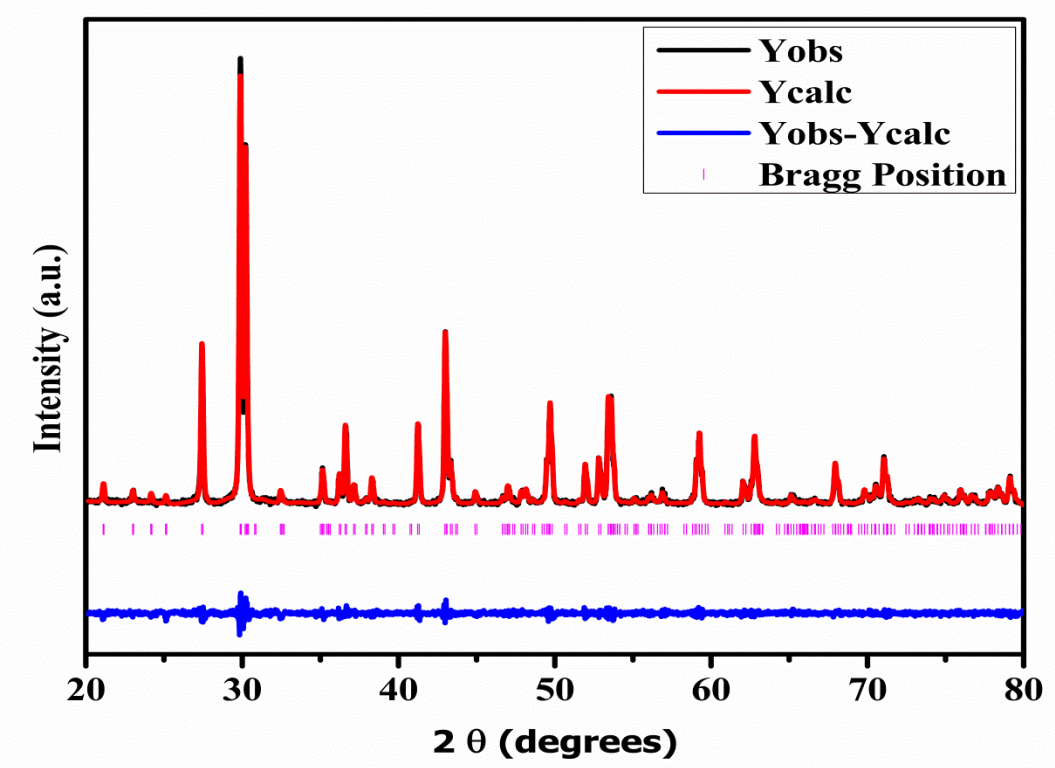

Figure 5.3 Rietveld refinement of XRD data for $Ba_6Y_2Ti_4O_{17}$ ceramic sintered at 1400 ^{0}C for 24 h

The refined structural parameters are listed in Table 1. The observed lattice parameters are very close to earlier reported hexagonal perovskite structure [Kuang *et al*. (2002)].

Table 5.1 Rietveld refined structural parameters of $Ba_6Y_2Ti_4O_{17}$ ceramic

Atom	X	Y	z
Y	0	0	0.12558
Ba1	0	0	0
Ba2	2/3	1/3	0.08716
Ba3	1/3	2/3	0.18273
Ba4	0	0	1/4
Ti1	2/3	1/3	-0.0538
Ti2	2/3	1/3	0.20299
O1	1/3	2/3	0.0038
O2	-0.3371	-0.1675	0.07681
O3	0.3495	0.17398	0.16956
O4	0.52120	0.04240	1/4

Space group: $P6_3/mmc$; $\chi^2 = 3.24$, Lattice parameters a = 5.92801 Å and c = 29.5218 Å

Figure 5.4 shows the FE- SEM image of fractured surface of BYTO ceramic sintered at 1400 ^{0}C. Figure 5.4 (a) shows the neat and clean hexagonal crystal formation whereas the highly magnified image Figure 5.4 (b) image clearly indicates the single hexagonal particle. Figure 5.4 (c) explains the EDX spectra which was recorded on the single hexagonal particle shows the presence of Ba, Y, Ti, and O elements which confirmed the elemental composition of the material. Figure 5.4 (d) indicates elemental mapping of BYTO ceramic every element has different color and their corresponding color bar is also mentioned.

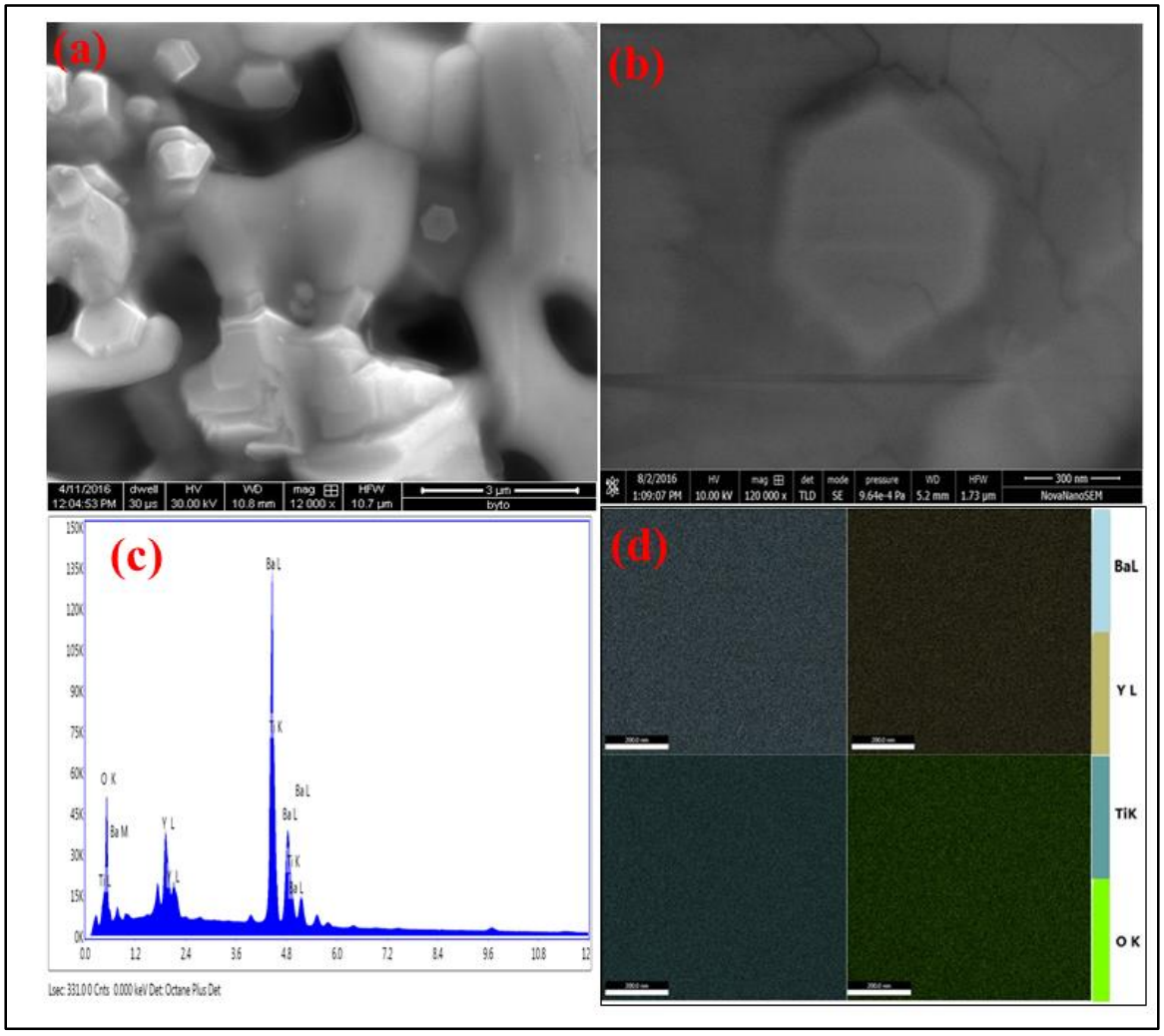

Figure 5.4 (a, b) SEM micrograph **(c)** EDX and **(d)** elemental mapping of BYTO ceramic sintered at 1400 ^{0}C for 24 h

The conclusion drawn from the mapping image is that the corresponding elements are uniformly distributed with their stoichiometric ratio that also showed the purity of material. The atomic percent of Ba, Y, Ti, and O obtained by EDX were found to be 31.6, 7.6, 11.9 and 48.9 respectively. The morphology of the hexagonal particles of BYTO ceramic also supported by bright field TEM image as shown in Figure 5.5 (a).

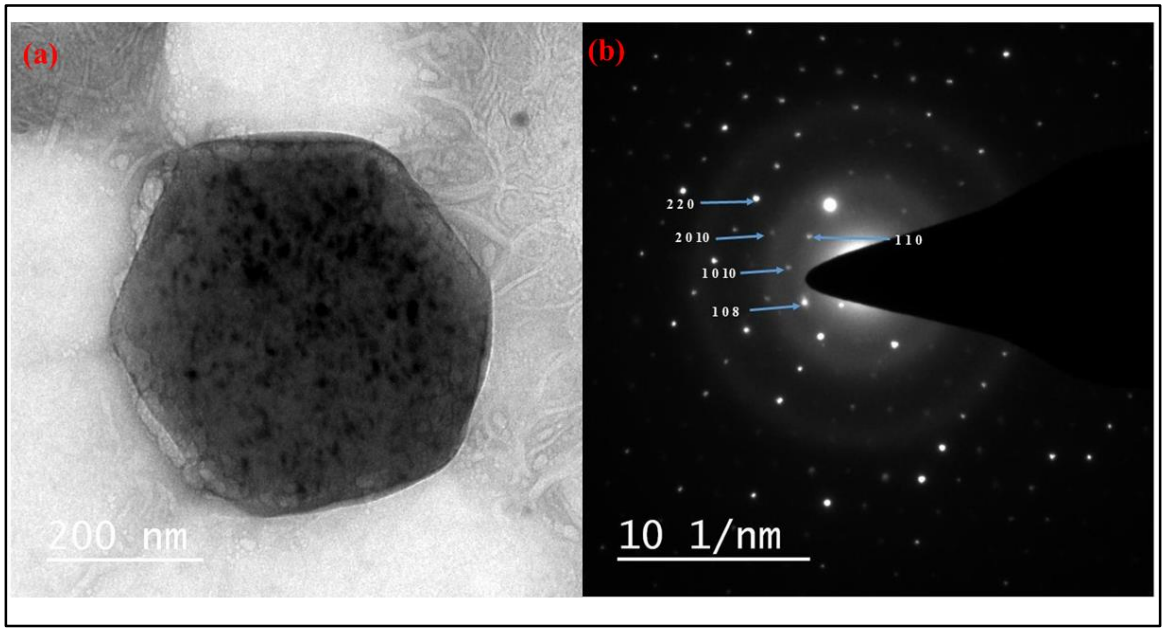

Figure 5.5 (a) Bright field TEM image and **(b)** Selected Area Electron Diffraction (SAED) Pattern of BYTO ceramic

The particle size was found to be 470 nm. Figure 5.5 (b) shows the selected area electron diffraction pattern (SAED) of the BYTO ceramic observed that parallel spot patterns indicate the single crystal nature of the material. The calculated inter-planer spacing 'd' obtained from TEM substantiate the result with XRD. Figure 5.6 shows the variation of polarization with electric field of BYTO ceramic at few selected temperatures measurement was done at frequency 200 Hz. The sample exhibited the polarization hysteresis loop which is the characteristic feature of ferroelectricity. The frequency dependent dielectric behavior also supports ferroelectric nature of BYTO ceramic [Belik *et al*. (2006)]. It is observed that the value of remanent polarization and coercive electric field decrease with temperature due to reverse effect of induced electric field and ferroelectric switching of dipoles with temperature [Huang *et al*. (2015), Patel *et al*. (2016)].

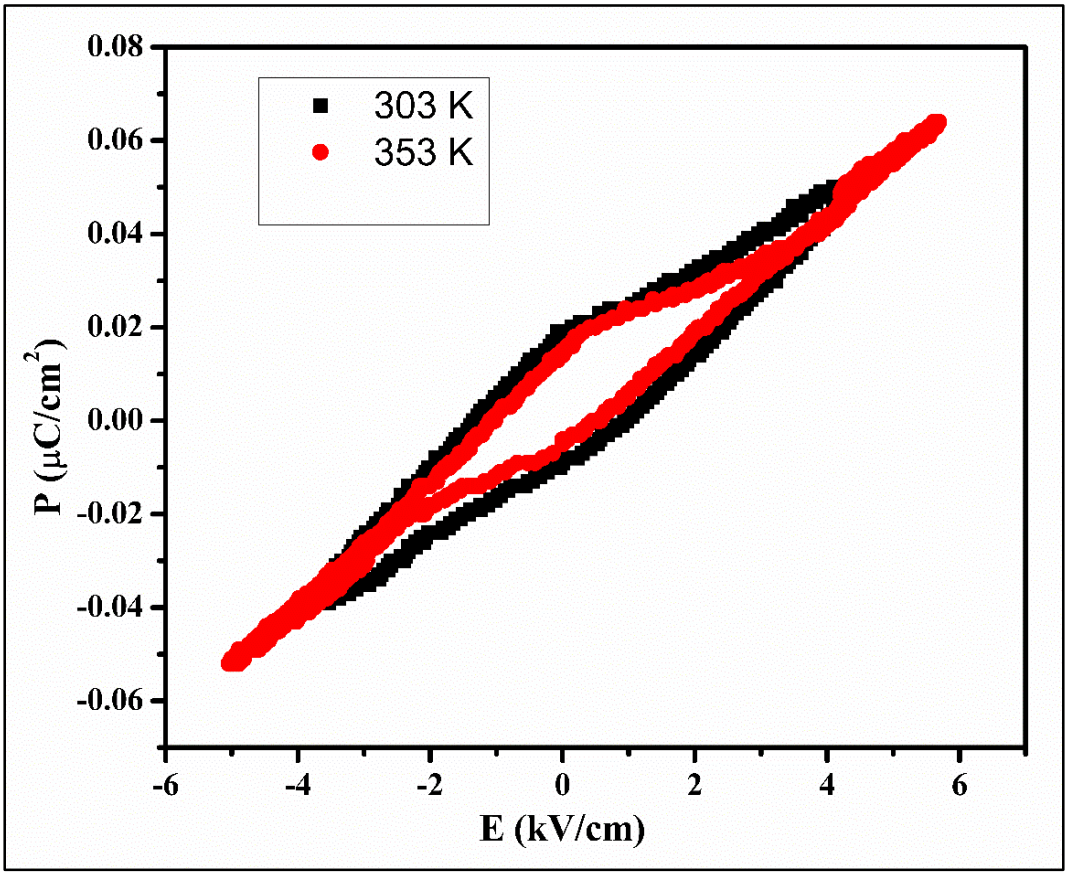

Figure 5.6 PE hysteresis loop of $Ba_6Y_2Ti_4O_{17}$ ceramic at 303 and 353 K

The observed remanent polarization and coercive field of the BYTO ceramic is very less as compared to earlier reported doped and un doped barium titanate may be happen due to the element Y occupy some site of Ti which suppress the off centre effect. The saturation polarization was not observed due to presence of oxygen vacancy, [Dutta *et al*. (2016)] lossy capacitor behavior and leakage current of BYTO ceramics [Yadava *et al*. (2016a)]. In order to investigate the magnetic behavior of BYTO ceramic, the magnetic measurements were done by MPMS magnetometer. Figure 5.7 shows the magnetization *versus* magnetic field measured at different temperatures 5 K, 50 K and 300 K.

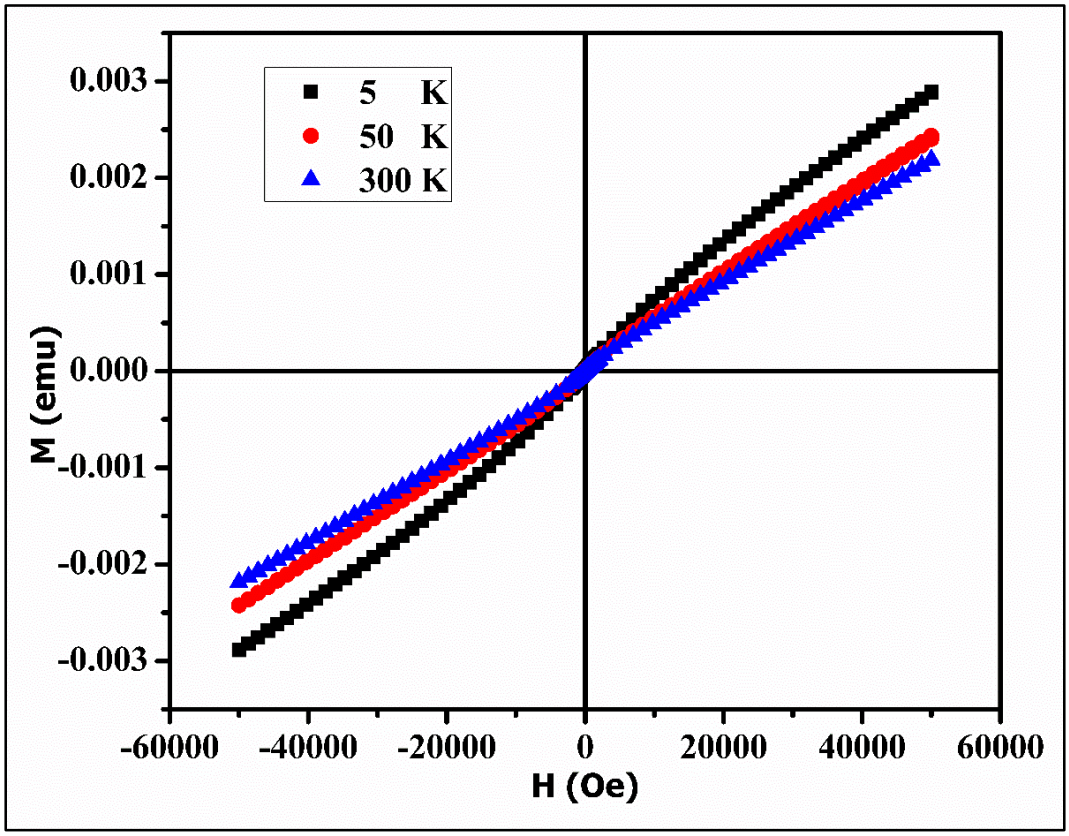

Figure 5.7 M-H hysteresis loop of BYTO at few selected temperatures

The recorded M-H hysteresis loop shows that on increasing temperature ferromagnetic behavior of BYTO shift towards paramagnetic behavior. The observed remanent magnetization (M_r) and coercive field (H_c) were also decreases with increasing of temperature that supports the ferromagnetic to paramagnetic transition. Such inverse relation of remanent magnetization with temperature may be due to the disordering of magnetic domains increases on increasing temperature [Nag *et al*. (2008), Toner *et al*. (2012)]. The temperature dependence magnetization (M-T) curve recorded at 4000 Oe is shown in Figure 5.8. The Field cooled (FC) and zero field cooled (ZFC) decreases simultaneously with increasing temperature from 5 to 20 K and then divergence of FC and ZFC observed at 75 K above which coincidence of curve

takes place. The broad peaks at 55 K represents blocking temperature (T_B) which indicates magnetic moments are frozen in different direction bellow blocking temperature [Maksutoğlu *et al*. (2015)]. Such low temperature divergence of FC and ZFC is generally present in frustrated magnetic system that indicates the ferromagnetic and antiferromagnetic interactions.

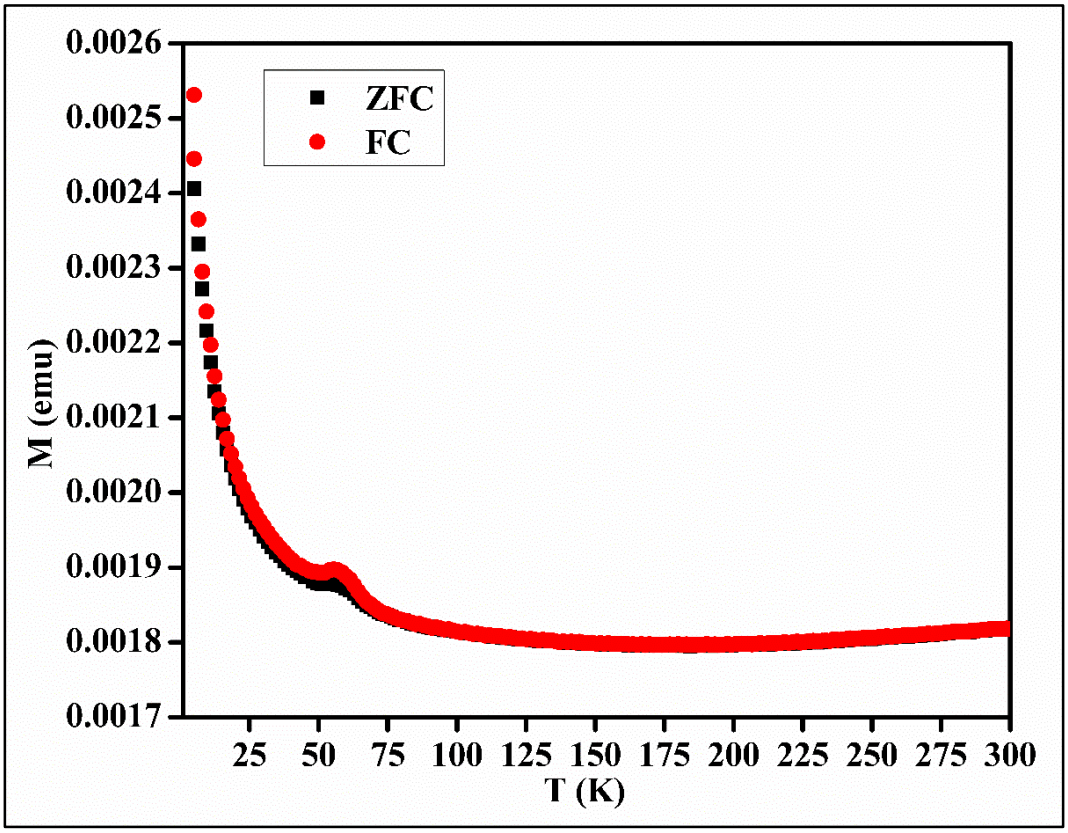

Figure 5.8 Temperature dependence of FC and ZFC magnetization for $Ba_6Y_2Ti_4O_{17}$ ceramic at 4 Tesla applied field

The plots of dielectric constant (ε_r) and dielectric loss (tan δ) versus frequency as well as temperature are shown in Figure 5.9 (a, b). The high value of dielectric constant towards low frequency region and at high temperature was attributed space charge polarization due to

accumulation of charge carrier at the electrode interface on applying electric field [Jonscher (1977), Zheng *et al*. (2014)].

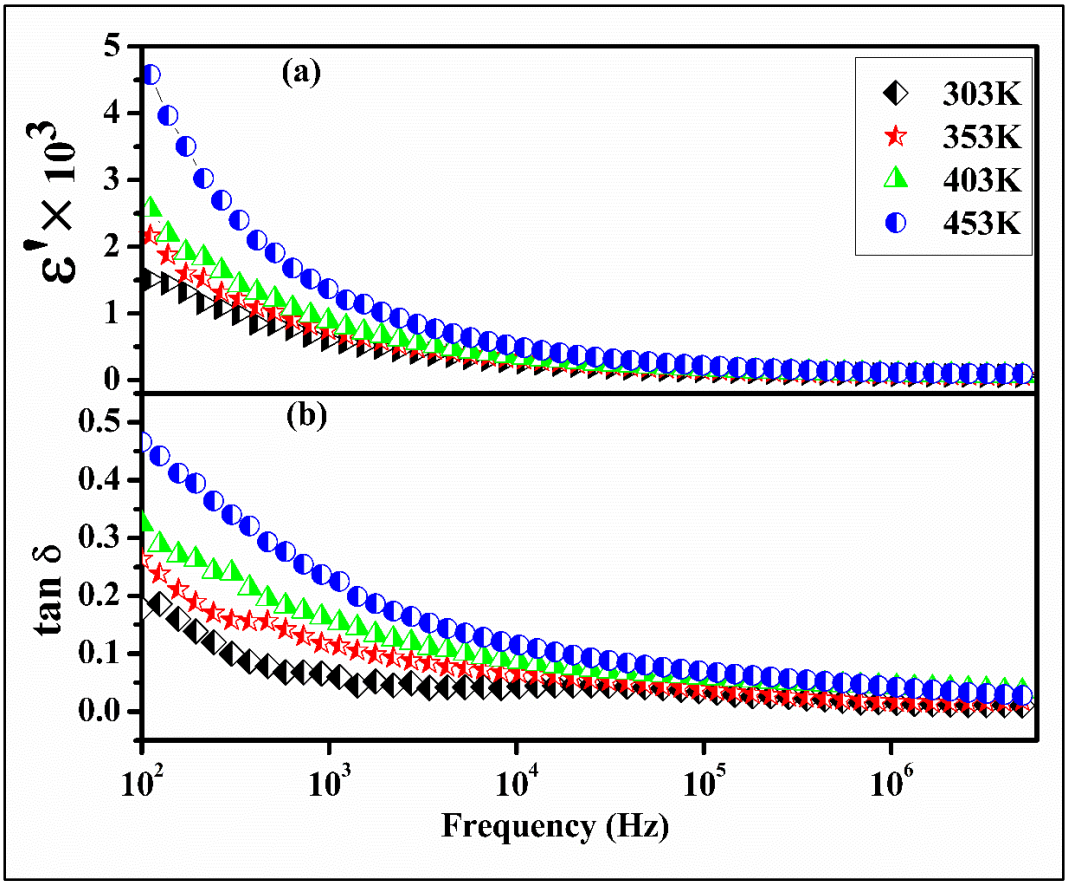

Figure 5.9 Variation of **(a)** Dielectric constant and **(b)** Dielectric loss (tan δ) with frequency of BYTO ceramic at few selected temperatures

The dielectric constant found to be 1.5×10^3 at temperature of 303 K and 100 Hz frequency. The high dependency of dielectric loss at lower frequency region may be due to small interfacial polarization in BYTO ceramic [Rai *et al*. (2012)]. The value of dielectric loss was calculated and found to be 0.20 at 303 K and 100 Hz. The temperature dependent dielectric constant (1000/ε') are shown in Figure 5.10 at 1 kHz.

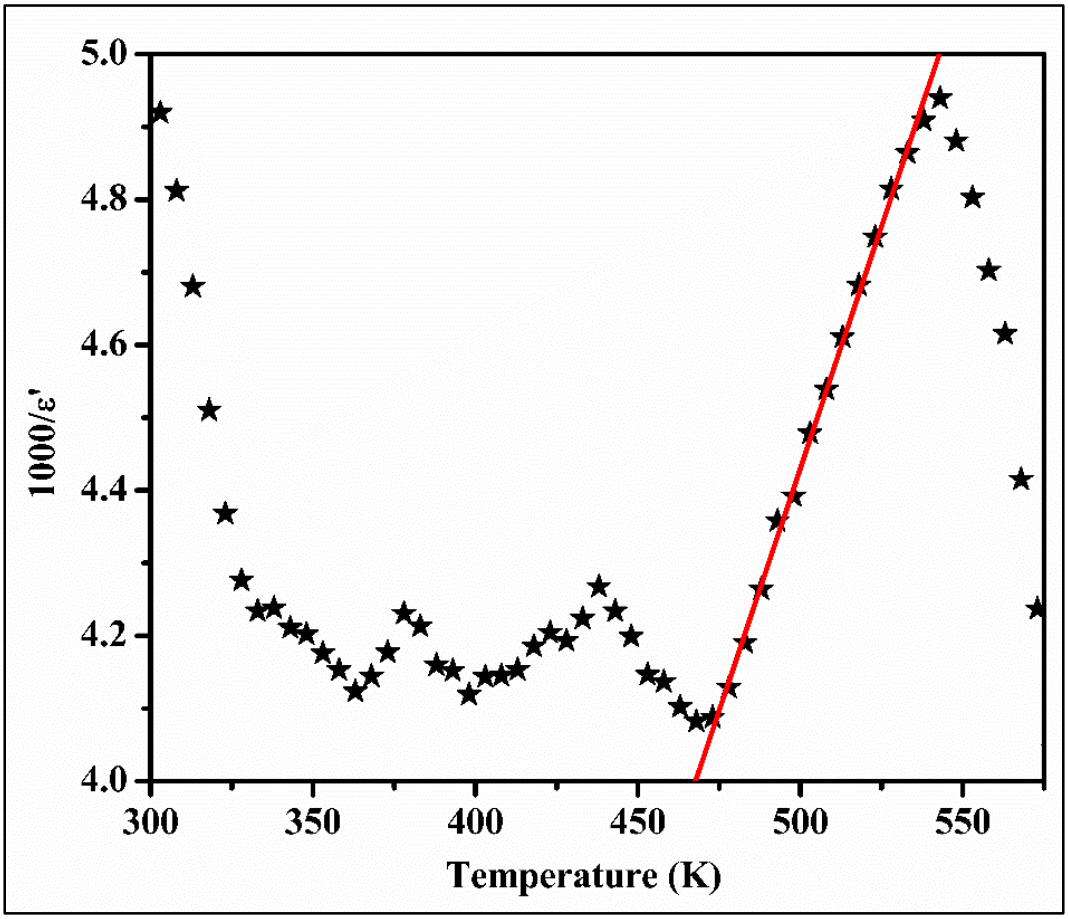

Figure 5.10 Plots of inverse of dielectric constant (1000/ε') of BYTO ceramic at 1 kHz with variation of temperature

The intercept on temperature axis of the fitted plot gives the value of Curie temperature (Tc). The calculated value of Tc was found to be 468 K [Liu *et al*. (2011)]. The complex impedance spectroscopy is also a valuable technique to investigate polarization mechanism in grain and grain boundaries of electro-ceramics. Figure 5.11 shows the cole - cole plot of BYTO ceramic at few selected temperature (303-453 K).

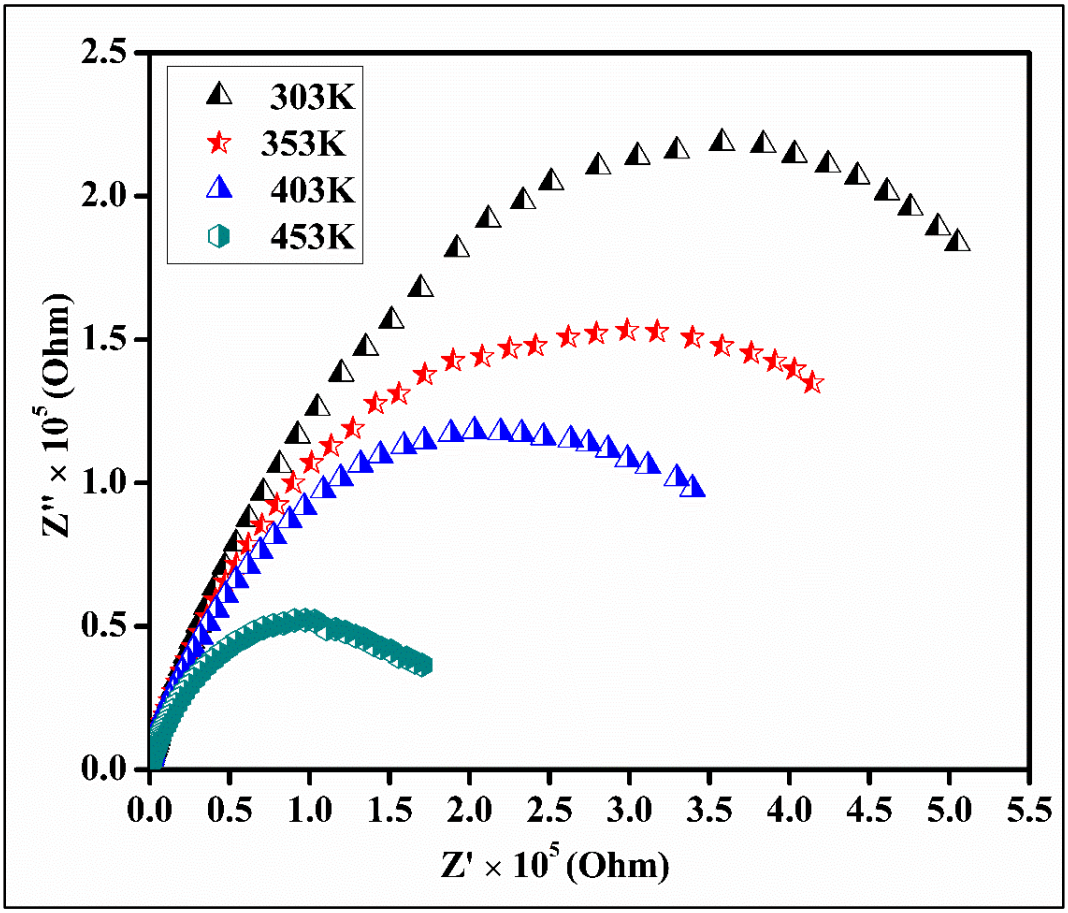

Figure 5.11 Impedance plane plot (Z'' Vs Z') of BYTO ceramic at few selected temperatures

The semi-circular arc represents the contribution from the grain boundary of the ceramic. The first intercept on real Z' axis was not zero as shown in highly magnified Figure 5.12 that indicates there is a possibility of another semi-circular arc at higher frequency region for grain contribution.

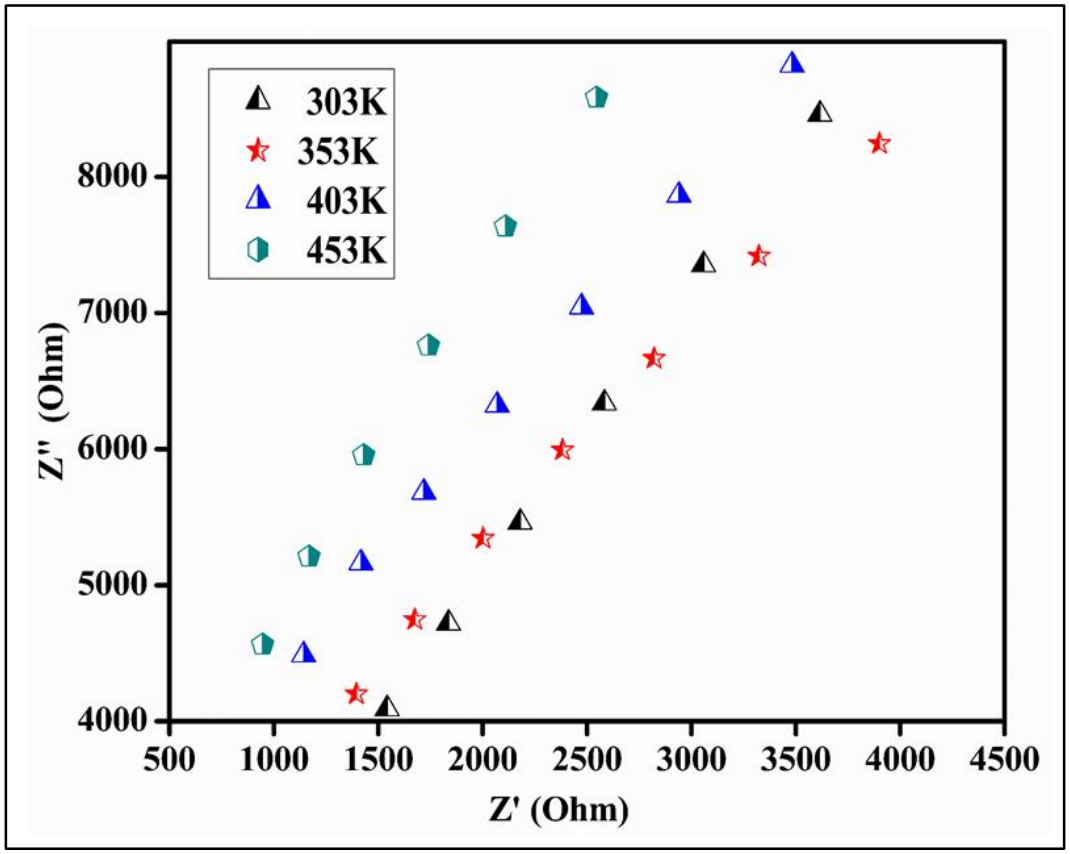

Figure 5.12 Expanded view of impedance plots at high frequency region close to the origin at few selected temperatures for BYTO ceramic

The extrapolated second intercept on Z' axis represents resistance of grain boundary [Sigh *et al*. (2013)]. The resistance of grains and grain boundaries at few temperatures was determined by formulae given in equation (5.5-5.7).

$$Z^* = \frac{1}{R_g^{-1} + i\omega C_g} + \frac{1}{R_{gb}^{-1} + i\omega C_{gb}} = Z' - iZ'' \qquad (5.5)$$

where,

$$Z' = \frac{R_g}{1+(\omega R_g C_g)^2} + \frac{R_{gb}}{1+(\omega R_{gb} C_{gb})^2} \quad (5.6)$$

and

$$Z'' = R_g \left[\frac{\omega R_g C_g}{1+(\omega R_g C_g)^2}\right] + R_{gb} \left[\frac{\omega R_{gb} C_{gb}}{1+(\omega R_{gb} C_{gb})^2}\right] \quad (5.7)$$

The calculated values of grain resistance were found to be (R_g) 1473, 1296, 911 and 760 ohm and grain boundary resistance (R_{gb}) 7.11×10^5, 5.76×10^5, 4.60×10^5 and 2.30×10^5 ohm at 303, 353, 403 and 453 K respectively. These data show that semiconducting and insulating nature of grains and grain boundaries that are also supported by internal barrier layer capacitor (IBLC) mechanism based on extrinsic factor as reported in previous literature which is responsible for the high dielectric constant values in ABO_3 perovskites [Sigh *et al*. (2014), Cao *et al*. (2015)]. On increasing temperature resistances of grains and grain boundaries were decreases that indicate the semiconducting behavior of material [Ullah *et al*. (2014)]. Figure 5.13 shows variation of the imaginary part of impedance with frequency at selected temperature.

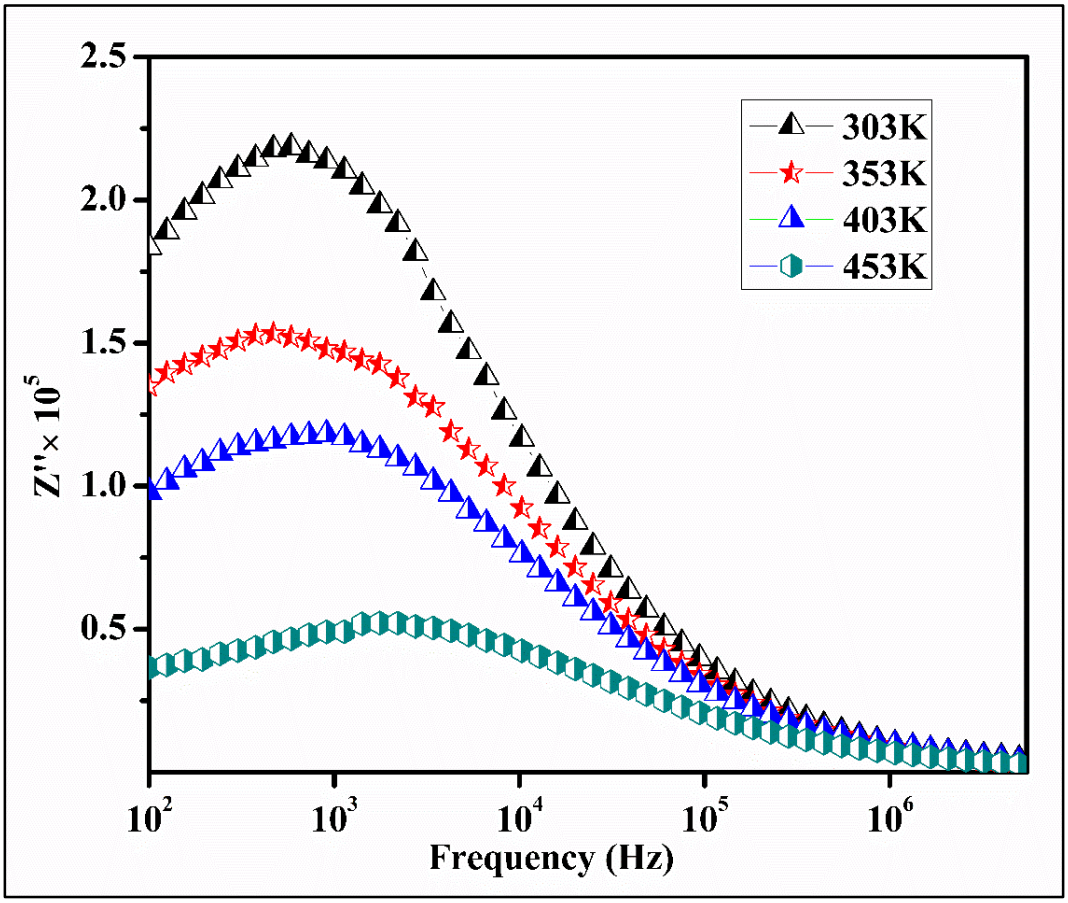

Figure 5.13 Variation of imaginary part of impedance (Z'') with frequency at few selected temperatures for BYTO ceramic

As observed from the figure that the height of peaks decreases and asymmetrical broadening of peaks increases with increase of temperature [Liu *et al*. (2012)]. At lower frequency region high broadening peaks were observed while at higher frequency the peaks are merged which substantiate the presence of temperature dependent electrical relaxation phenomena of BYTO ceramic.

5.4. Conclusions

BYTO ceramic was successfully synthesized using the semi-wet combustion route. XRD patterns clearly showed the presence of single phase of the ceramic sintered at 1400°C. The synthesized material shows the excellent dielectric, ferroelectric and magnetic properties. Hexagonal perovskite nature of BYTO describe by SEM, TEM and Rietveld refinement of XRD data. Magnetic hysteresis showed the existence of the paramagnetic behavior of the material on increasing temperature. PE hysteresis revealed that temperature dependent polarization and coercive electric field. The absence of saturation in both magnetic and ferroelectric hysteresis indicates lossy behavior of material. The high dielectric constant and low tangent loss indicates the importance of BYTO towards microelectronic devices.